Feature Extraction of Wood-Hole Defects Using Empirical Mode Decomposition of Ultrasonic Signals

Mohsen Mousavi[a], Mohammad Sadegh Taskhiri[b], Damien Holloway[a,1], J.C. Olivier[a], Paul Turner[b]

[a] *School of Engineering, University of Tasmania, Hobart 7005, Tasmania, Australia*
[b] *ARC Centre for Forest Value, Discipline of ICT, College of Sciences and Engineering, University of Tasmania, Australia.*

Abstract

Holes and knots are common defects that occur in wood that affect its value for both structural and high-end aesthetic applications. When these defects are internal to wood they are rarely evident from visual inspection. It is therefore important to develop techniques to detect and analyse these defects both in standing trees prior to harvesting them and in processed timber and/or completed wooden structures. This paper presents an effective method to detect and analyse hole defects in wood. The method uses the recorded output wave signal from an ultrasonic device tested on rectangular wood samples. The ultrasonic wave signal is decomposed into its constructive modes using Empirical Mode Decomposition (EMD). This process decomposes a non-stationary non-linear wave signal into its semi-orthogonal bases known as intrinsic mode functions (IMFs). A matrix of all IMFs (except the residual IMF) is then assembled and its covariance matrix derived. The research demonstrates through several experimental studies that the maximum eigenvalue of the proposed covariance matrix is more sensitive to hole defects in wood than traditionally used measures such as time-of-flight. The results provide evidence that the proposed damage sensitive feature (DSF) can successfully detect hole defects in hardwood samples but further work is recommended on its application to other materials. It is anticipated that this method will have wide applicability in the forestry and timber industries for aiding in product value determination.

Keywords: `Ultrasonics, Empirical Mode Decomposition, Damage detection, Nondestructive testing, Wood, Damage sensitive feature, Defects, Time-of-flight`

Email address: `Corresponding author: damien.holloway@utas.edu.au` (Damien Holloway)

1. Introduction

Wood has been employed as a construction material for centuries due to its relatively high strength to weight ratio, its good heat and electrical insulation properties, and its workability, enabling simpler and faster construction [1, 2]. Wood continues to be widely used in construction – for example, more than 80% of the total power utility poles used in Australia continuing to deploy wood i.e., more than five million timber poles in total [3].

In terms of mechanical properties, wood is characterised as an orthotropic material with independent mechanical properties in three mutually perpendicular axes, i.e. longitudinal, radial, and tangential [4]. Usually these mechanical properties of wood are determined by static tests with wood samples taken from harvested and processed trees [5].

However, many wood defects are generated during the growth of the standing tree pre-harvest. A common defect in trees results from a standing tree not being pruned and undergoing a process of natural self-pruning, leaving dead stubs that the tree subsequently grows around or over. These processes create internal defects such as knots and holes internal to the tree. To accurately detect and analyse these defects to differentiate between a healthy versus defective trees requires the use of either destructive or non-destructive damage testing (NDT) techniques.

Moreover, wooden materials may also deteriorate while in service as structural elements due to either biological (such as decay, fungi, and termites) or physical (climatic such as rain and sun) processes [6]–some of these defects are also internal. In recent years, issues such as the preservation of wooden architectural heritage has increased demand for NDT approaches to monitor the internal health condition of historic wooden structures [7, 8, 9].

In general a NDT technique has two key components: a sensing technology to record signals from a structure, and a damage detection algorithm to derive information about the health condition of the structure from the signal.

Many different sensing technologies have been used by researchers for damage evaluation of wood materials [10]. These include ultrasonics, radiography [11] and thermography [12], however, ultrasonic testing seems to be the most promising and widely used approach. This is mainly due to the fact that an ultrasonic test is less harmful for the wood (and the human operator) and is relatively less expensive [13]. It has also been proven that the ultrasonic waves are sensitive to many wood characteristics such as density, stiffness, strength, grain orientation, moisture content, as well as defects such as cracks, knots, and insect damage [14].

The application of ultrasonic techniques for evaluation of wooden material has been reported by a number of researchers [15, 16, 17, 18, 19, 20]. This includes detection of artificial defects as reported in [6, 16]. Several well-known ultrasonic systems have been used for condition

monitoring of wooden materials, including electromagnetic ultrasonics [21], laser ultrasonics [22], and air-coupled ultrasonics (ACU) [23, 24, 25, 26]. However, there are some shortcomings with each one when dealing with defects in wood sections. For instance, electromagnetic ultrasonics is more robust when used in conductive material evaluation, while laser ultrasonics devices tend to be expensive. Chimenti et al. noted that ACU is effective for evaluation of low density materials such as paper, wood, and carbon-reinforced composites. A reason for this could be due to the smaller impedance difference between such materials and air [25]. However, Fang et al. argued that ACU-based techniques suffer from low quality ACU signals and thus more advanced signal processing techniques need to be used for these methods [24]. As such, the application of contact ultrasonic devices still seems promising. This paper is focused on the application of contact-ultrasonic systems.

In terms of signal processing algorithms, the Hilbert-Huang transform (HHT) has been widely used in the context of structural health monitoring [27, 28] since the empirical mode decomposition (EMD) algorithm was first introduced by Huang et al. [29]. In fact the EMD algorithm has been employed as an effective method for fault diagnosis in a variety of other scientific fields [30, 31]. It is well-known that EMD is an adaptive and approximately orthogonal filtering process. This characteristic has been used by some researchers. For instance, Liu et al. proposed a special version of EMD for image processing called directional empirical mode decomposition (DEMD) for texture classification problems [32]. The process of extracting features using EMD thus is a well-developed field in the literature.

HHT and EMD have been used in many applications of ultrasonic signals as well. For instance, Sun et al. proposed a denoising method for laser ultrasonic signals based on the criterion of consecutive mean square error using EMD [33] as a useful approach to reducing the aliasing between useful signals and noise. Therefore, using this property of EMD, Yu et al. proposed a time-windowing method with a kurtosis test strategy considering the multi-mode and broadband characteristics of laser ultrasonic signals for denoising [34]. Chen et al. proposed a novel approach to identify the arrival time of overlapping ultrasonic echoes in time-of-flight diffraction (TOFD) flaw detection [35]. As such, the authors applied EMD to decompose a non-stationary non-linear ultrasonic signal into its constructive IMFs. Zhang et al. used EMD for feature extraction of flaw signals [36]. These authors related time domain and frequency domain of IMFs to flaw information.

In this paper, Section 2 presents a new DSF for hole-damage feature extraction, using an ultrasonic signal that is recorded through ultrasonic tests on wooden sections. The results show that this performs better than the traditional time-of-flight method. The approach presented

involves the non-stationary non-linear ultrasonic signal being first decomposed into its IMFs using EMD. Second, the matrix of all IMFs (except the residual IMF) is constructed and its covariance matrix is obtained. The paper demonstrates through different experimental studies that the largest eigenvalue of the covariance matrix is a useful feature able to characterise hole defects in wood materials. Results are presented for both parallel and perpendicular to grain signal transmission.

2. Proposed damage sensitive features

A new damage sensitive feature (DSF) is proposed in this paper that is derived from the ultrasound signal obtained in the tests described in Section 3, i.e. briefly, from the time records of an ultrasonic pulse transmitted through the timber sample in either the radial or tangential direction. The proposed DSF is based on the intrinsic mode functions (IMFs) of the signal, which are simple but non-stationary sine-like oscillatory components into which a signal is decomposed following empirical mode decomposition (EMD). We therefore first briefly describe EMD, then define the DSF.

2.1. Empirical mode decomposition (EMD)

The EMD algorithm was first introduced by Huang et al. in order to decompose a non-stationary, non-linear signal into its constructive oscillation modes (IMFs) [29]. Unlike the Fourier basis functions, IMFs can be non-linear and non-stationary, i.e. they can contain modulation of both amplitude and frequency with time. However, as with linear modal analysis, each IMF is narrow band and only involves one mode of oscillation, so over short time windows they can be considered to be loosely sinusoidal in form. Therefore, the concepts of instantaneous frequency and amplitude are well defined for IMFs. Hence, the IMF's characteristics can be summarized as follows:

1. Each IMF is narrow band, and it involves only one mode of oscillation.
2. An IMF can be non-stationary.
3. Each IMF is modulated in both amplitude and frequency.

The flowchart of the basic EMD algorithm applied to an arbitrary signal $X(t)$ is shown in Figure 1. However, one can easily decompose a signal $X(t)$ in MATLAB (version 2018a onward) with the function `emd` as follows,

$$[\mathtt{V}, \mathtt{r}] = \mathtt{emd}(\mathtt{X}); \tag{1}$$

where V is a matrix containing all the IMFs except the residual IMF, which is stored in the vector r.

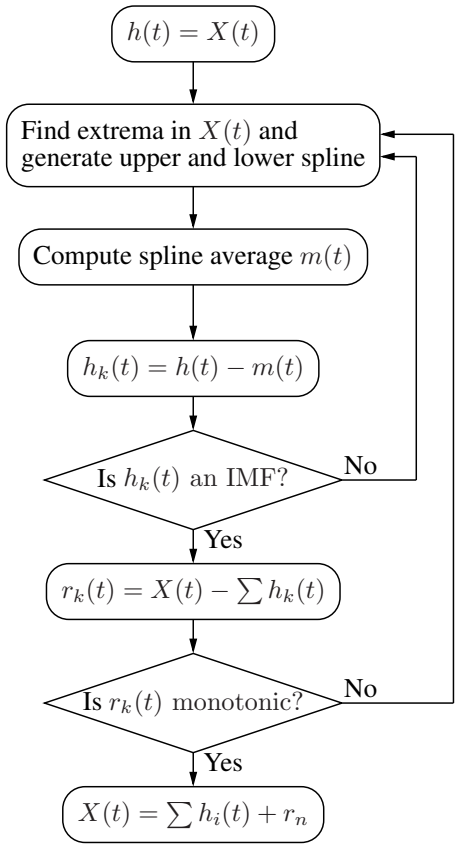

Figure 1: Flowchart for the EMD algorithm.

2.2. Proposed damage sensitive feature (DSF_1*)*

A damage sensitive feature is first proposed that exploits the matrix of IMFs extracted from a scattered ultrasonic wave to characterise hole defects in wood structures. We will show that the covariance matrix can be deployed. The intuition behind this comes from the fact that the maximum eigenvalue of the covariance matrix shows many interesting properties, making it a good DSF for the purpose of defect detection [37]. For instance, it is well-known that the maximum eigenvalue of the covariance matrix corresponds to the eigenvector that has a direction along which the data set has the maximum variance. Therefore, it is able to characterise properties of the ultrasonic signal.

The covariance matrix is constructed from the recorded ultrasonic signal from an ultrasonic test conducted on wooden samples. However, the obtained signal is a time series which first needs to be decomposed into its constructive modes of oscillation to form the matrix of IMFs, of which the modes are columns. Once the covariance matrix corresponding to the matrix of IMFs is constructed, we seek its maximum eigenvalue. Hence the procedure of the proposed feature extraction technique using the ultrasonic signal $S(t)$ obtained from an ultrasonic test can be described as follows:

1. First normalise the signal $S(t)$ recorded from the ultrasonic test on the sample to have a zero mean and unit maximum peak to trough range as follows,

$$\tilde{S}(t) = \frac{S(t) - \mu}{S_{\max} - S_{\min}} \tag{2}$$

where μ, $S_{\max}$ and $S_{\min}$ represent respectively the mean, maximum and minimum of the signal $S(t)$. The normalisation eliminates the gain effect existing in each IMF component produced from the EMD decomposition of the ultrasound signal [38]. We designate the normalised version of signal $S(t)$ as $\tilde{S}(t)$.

2. Use the EMD algorithm to decompose the signal $\tilde{S}(t)$ into its constructive IMFs and stack them all in matrix V of IMFs (see Equation 1). Note that V is a matrix with size $m \times n$ where m is the number of samples in the time series and $n \ll m$ is the number of modes extracted by EMD.

3. Compute the covariance matrix corresponding to the matrix $V_{n\times m}$. For this, one may either compute $C^{(1)}_{m\times m} = V \times V^{\mathrm{t}}$ or $C^{(2)}_{n\times n} = V^{\mathrm{t}} \times V$, in which $^{\mathrm{t}}$ represents the matrix transpose. To decide which covariance matrix to use, consider a lemma in linear algebra [39] (stated here without proof):

Theorem 1: *Let A and B be respectively $m \times n$ and $n \times m$ matrices where $n \leq m$. Then, the n eigenvalues of BA are identical to the first n eigenvalues of AB, with the additional eigenvalues being zero.*

Thus by considering $A = V$ and $B = V^{\mathrm{t}}$, it follows that the n eigenvalues of $C^{(2)}$ are equal to the first n eigenvalues of $C^{(1)}$, with the additional eigenvalues of $C^{(1)}$ being zero. Clearly therefore either can be used, and we choose $C^{(2)}$ because the size of $C^{(2)}_{n\times n}$ is vastly smaller than the size of $C^{(1)}_{m\times m}$ ($n \ll m$).

4. Find the maximum eigenvalue of the covariance matrix $C^{(2)}$ and nominate it as a feature for characterising wood condition. Note that this can be done in MATLAB using the instruction `max(eig(C))`.

In the following sections, we test the following hypothesis:

Hypothesis 1: *The largest eigenvalue of the covariance matrix corresponding to the decomposed acoustic signal through EMD is sensitive to hole defects in wooden materials.*

As such the DSF_1 is defined as follows,

$$\mathrm{DSF}_1 = \max\left(\mathrm{eig}\left(C^{(2)}\right)\right) \tag{3}$$

2.3. Filtering the noise (DSF_2*)*

It is noted that the detected ultrasonic signal is somewhat contaminated by noise, which can be evident in the first IMF. Therefore, in order to test the sensitivity of the proposed DSF to noise a low pass filter with the cutoff frequency of 500 kHz has been applied to the measured data. For the current setup (see Section 3) this is an order of magnitude above the transmitted pulse frequency (54 kHz), and more than an order of magnitude below the sampling frequency (10 MHz) used by the receiver to detect the ultrasonic signal. This filtered signal is then used for damage detection in exactly the same manner as the unfitered signal. Accordingly, in this paper the damage detection results using the unfiltered ultrasonic signal is denoted DSF_1 while the results derived from the filtered signal are denoted DSF_2.

3. Experimental setup

To test the damage detection methods proposed above in Section 2, ultrasonic tests were conducted on wood samples of dimensions $300 \times 90 \times 90$ mm^3, with and without introduced defects. Figure 2a shows schematically how the transducers were set up with respect to the sample, and the artificial defect can be seen in the form of a hole of diameter D drilled through the full thickness of the sample, approximately at the centroid of the rectangle.

The ultrasonic device (Pundit PL200) used for conducting the ultrasonic tests is shown in Figure 2b. The device emits short 17.5 μs sinc-like (i.e. $\sin(x)/x$ including a single peak) impulses. The manual states "transducers supplied with the instrument are not damped and, therefore, on being excited by the transmitter they have a long ring-down time." Therefore the signal that is transmitted into the sample can be assumed to be a lightly damped impulse response, but the pulse repetition frequency is several orders of magnitude lower than the transducer resonant frequency, preventing mixing of transmitted and returned pulses. To operate the Pundit PL200 it must be set to one of a limited number of user-specified frequencies (24, 54, 150, 250 or 500 kHz) that must conform to the operational frequency of the selected transducer pair. For the current work the 49.7 mm diameter 54 kHz transducer (part number 325 40 131) was used and the receiver gain was set to the device's '1 dB' setting. The gain is set following some trial runs such that the signal is strong but does not saturate. The probing wave type is a P-wave (compressional wave) with transducer voltage 50 V.

In order to ensure good contact between the transmitter and receiver and the surface of the wood, an ultrasonic couplant gel (Proceq Ultraschall-Koppelpaste) was used on both transmitter and receiver surfaces. As this is intended to be a practical test that can be carried out in the field a method of obtaining reliable results without having to precisely measure the contact

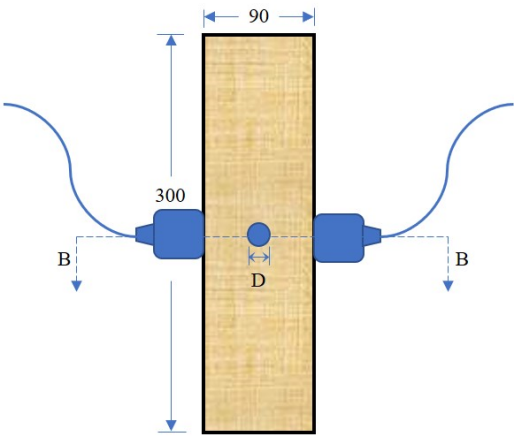

(a) Schematic of test

(b) Ultrasonic device (Pundit PL 200)

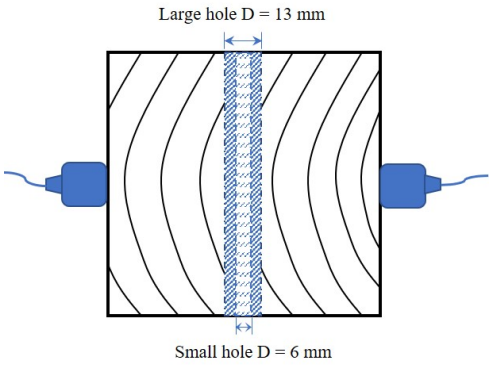

(c) Radial test (B-B)

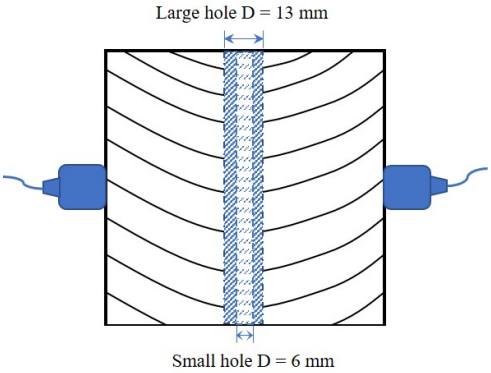

(d) Tangential test (B-B)

Figure 2: Ultrasonic test experimental set-up.

pressure was sought. Firm pressure with sufficient gel ensured that there was a complete layer of gel between the sample and transducer with contact over the whole area. Excessive pressure, or even maintaining pressure with some unavoidable movement, tended to squeeze out the gel, compromising the integrity of the contact. If in doubt, some additional gel was added, which always restored good contact when lost. Maintaining sufficient gel was more critical than the pressure used.

To evaluate the contact procedure, approximately 50 replicates of each ultrasound test were conducted, and the wave form and reported wave velocity were carefully monitored in order to verify that consistent contact between probes and samples had been achieved. Provided that contact was good these were highly consistent and the exact amount of pressure used did not appear to affect results, whereas any records for which the wave form or reported wave velocity were anomalous were discarded. Effects of minor variations in signal strength were removed during processing by the signal normalisation of Equation 2.

The wave velocity was calculated by the Pundit PL200 device from the time of flight, measured by the Pundit PL 2100, and a distance between transducers entered by the user. Time of flight is determined by the Pundit PL 200 by detecting the time at which return wave exceeds a preset threshold—the device's default threshold was used in the present work. The distance was measured using a tape meter placed on the top of the billet. Although literature shows the potential influences of moisture contents on ultrasound signals [40], in this work the test specimens were all cut from fully seasoned commercially available boards, so it is assumed the moisture content was consistent between samples and equal to the equilibrium moisture content (typically 10–15% for the local climate).

Four types of tests were carried out as follows:

1. ultrasonic wave transmission in the radial direction (perpendicular to the growth rings) on the intact specimens;
2. ultrasonic wave transmission in the radial direction with hole defects of diameter 6 mm or 13 mm introduced in the tangential direction (Figure 2c);
3. ultrasonic wave transmission in the tangential direction (parallel to the growth rings) on the intact specimens; and
4. ultrasonic wave transmission in the tangential direction with hole defects of diameter 6 mm or 13 mm introduced in the radial direction (Figure 2d).

First, to provide a baseline for the proposed DSF in each testing direction, the specimens were tested in the intact form with the ultrasound wave transmission in both the radial and tangential direction. Then the small (6 mm diameter) holes were drilled in the radial direction

in half the samples and in the tangential direction in the other half, and the samples were retested with wave transmission in the direction perpendicular to the hole. The same holes were then further drilled out to a diameter of 13 mm and the samples tested a final time, again with wave transmission perpendicular to the hole. With each specimen and testing configuration, 50 replicates of the ultrasonic tests were conducted to investigate the repeatability of the test and (as mentioned above) to evaluate the method of contact between specimens and transducers. The results were transmitted to laptop through PL-Link software. The raw data were exported to an Excel file for further signal processing using Matlab.

The test was conducted in normal room conditions with limited temperature fluctuations due to air-conditioned (20–22°C). They were conducted in a Tasmanian spring in moderate weather condition with a temperature range (15–23°C) and an average humidity level was normal at around 60%).

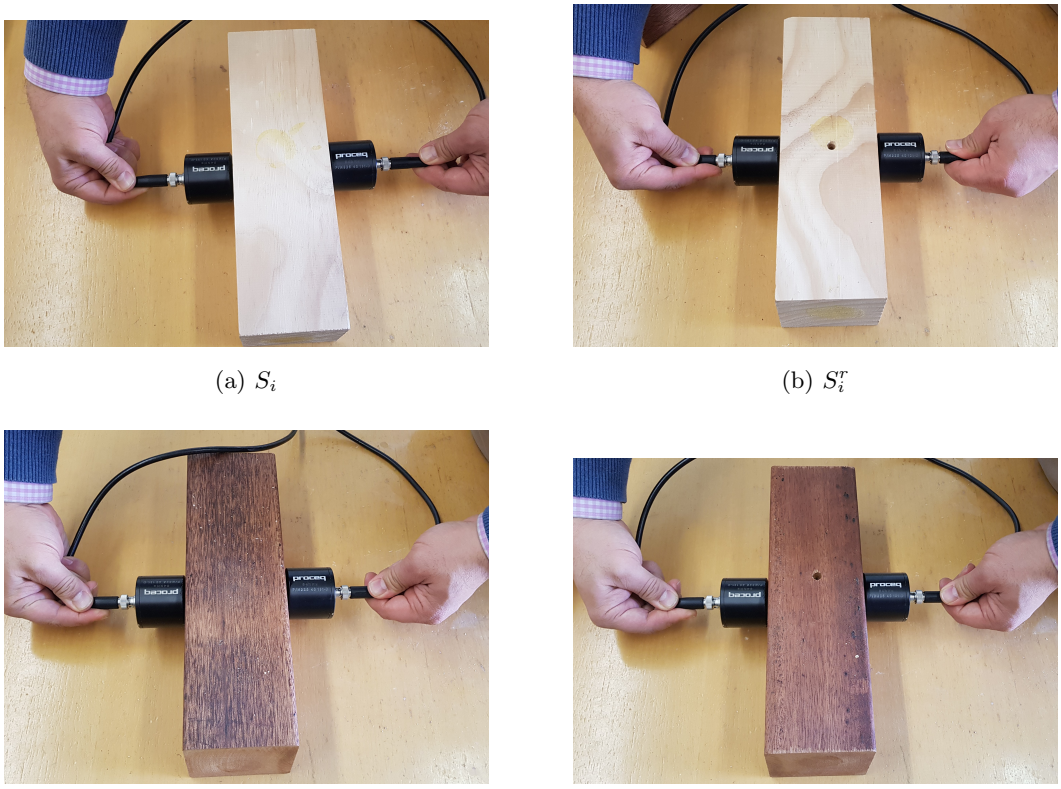

(a) S_i (b) S_i^T

(c) H_i (d) H_i^t

Figure 3: Different combinations of softwood/hardwood, and damaged/healthy, were tested—refer to keys in Table 1 for sample configurations.

The tests were conducted on two types of wood: a softwood (Radiata pine or pinus radiata, nominal density of 400 kg/m^3, Figures 3a and 3b) and a hardwood (merbau or instia palembanica , nominal density of 850 kg/m^3, Figures 3c and 3d). Samples were fully seasoned and assumed

to be at equilibrium moisture content for the conditions. However, since timber is a natural material, six specimen of each species were tested in this paper to establish the expected variability. These were designated S_1–S_6 and H_1–H_6 for the pine and merbau specimens respectively. Additional, a set of merbau specimens with natural radial cracks was tested, designated C_1–C_6. Superscripts r and t on specimens with introduced holes indicate whether the specimens were damaged in the radial or tangential direction respectively. In total, twelve conditions were tested on specimens as listed in Table 1 and shown in Figure 3. It is assumed that the nominal ultrasonic wave path (the direct line between transmitter and receiver) passed directly over the defect in both tangential and radial directions.

Table 1: Tests were conducted for the twelve conditions shown. 'NC' indicates there were natural radial cracks present. The sample designation is constructed using the code S, H or C for softwood, hardwood or hardwood with natural radial cracks; subscripts 1–6 to indicate replicates of nominally identical conditions; and superscripts t or r on only the damaged specimens to indicate the axis of the hole defect as being tangential to the growth rings or in the tree's radial direction.

Sample	**Softwood**	**Hardwood**	**Healthy**	**Introduced hole damage**	**Test wave direction**
$S_1 - S_6$	✓	-	✓	-	Radial
$S_1 - S_6$	✓	-	✓	-	Tangential
$S_1^t - S_3^t$	✓	-	-	Tangential	Radial
$S_4^r - S_6^r$	✓	-	-	Radial	Tangential
$H_1 - H_6$	-	✓	✓	-	Radial
$H_1 - H_6$	-	✓	✓	-	Tangential
$H_1^t - H_3^t$	-	✓	-	Tangential	Radial
$H_4^r - H_6^r$	-	✓	-	Radial	Tangential
$C_1 - C_6$	-	✓	NC	-	Radial
$C_1 - C_6$	-	✓	NC	-	Tangential
$C_1^t - C_3^t$	-	✓	NC	Tangential	Radial
$C_4^r - C_6^r$	-	✓	NC	Radial	Tangential

4. Results and discussion

4.1. General observations on damage measures

Tables 2, 3 and 4 show the calculated values for the proposed DSFs, along with the time of flight and the effective velocity of the ultrasonic wave propagation. The left halves of the tables present results for testing in the radial direction, and include results for specimens with holes

Table 2: Calculated DSFs for hardwood specimens (merbau) (V^r/V^t = ratio of radial to tangential velocity)

.

No introduced defect										
Sample	Radial wave testing direction				Sample	Tangential wave testing direction				V^r/V^t
	t_f (μs)	V (m/s)	DSF_1	DSF_2		t_f (μs)	V (m/s)	DSF_1	DSF_2	
H_1	47.6	1891	64.48	51.94	H_1	56.6	1590	45.68	61.89	1.19
H_2	49.2	1829	57.81	63.42	H_2	56.3	1599	65.67	76.71	1.14
H_3	49.5	1818	60.52	62.75	H_3	57.2	1573	53.93	57.64	1.16
H_4	49.4	1822	55.81	61.66	H_4	57.3	1571	56.51	58.96	1.16
H_5	49.2	1829	54.85	47.75	H_5	56.3	1599	52.03	64.87	1.14
H_6	49.6	1815	56.16	55.84	H_6	57.5	1565	48.14	57.02	1.16
μ	49.08	1834	58.27	57.23	–	56.87	1583	53.66	62.84	1.16
σ	0.74	28.50	3.63	6.45	–	0.53	15.03	7.06	7.39	0.02
Small (6 mm) diameter hole defect										
H_1^t	48.4	1860	75.95	86.34	H_4^r	57.9	1554	96.66	103.41	n/a
H_2^t	49.8	1807	81.63	86.33	H_5^r	57.7	1560	88.98	94.50	n/a
H_3^t	50.0	1800	85.13	86.47	H_6^r	58.3	1544	101.67	103.11	n/a
μ	49.4	1822	80.90	86.38	–	57.97	1553	95.77	100.34	–
σ	0.87	32.81	4.63	0.08	–	0.31	8.08	6.39	5.06	–
Large (13 mm) diameter hole defect										
H_1^t	48.4	1860	123.23	128.80	H_4^r	57.2	1573	128.29	132.92	n/a
H_2^t	50.0	1800	143.13	152.51	H_5^r	57.0	1579	109.93	127.59	n/a
H_3^t	50.0	1800	107.03	125.04	H_6^r	58.5	1538	100.95	107.72	n/a
μ	49.47	1820	124.46	135.45	–	57.57	1563	113.06	122.74	–
σ	0.92	34.64	18.08	14.89	–	0.81	22.14	13.94	13.28	–

Table 3: Calculated DSFs for hardwood (merbau) specimens with natural cracks (V^r/V^t = ratio of radial to tangential velocity).

No introduced defect										
Sample	Radial wave testing direction				Sample	Tangential wave testing direction				V^r/V^t
	t_f (μs)	V (m/s)	DSF_1	DSF_2		t_f (μs)	V (m/s)	DSF_1	DSF_2	
C_1	48.5	1856	41.32	35.58	C_1	51.6	1744	62.32	71.35	1.06
C_2	47.6	1891	48.73	43.46	C_2	50.7	1775	53.21	38.04	1.07
C_3	47.9	1879	44.51	40.43	C_3	51.3	1754	52.60	75.40	1.07
C_4	48.4	1860	40.72	34.91	C_4	51.1	1761	70.96	74.18	1.06
C_5	47.8	1883	46.75	40.04	C_5	50.5	1782	74.50	78.48	1.06
C_6	47.9	1879	49.32	46.41	C_6	50.4	1786	68.41	50.18	1.05
μ	48.02	1875	45.23	40.14	–	50.93	1767	63.67	64.61	1.06
σ	0.35	13.69	3.67	4.44	–	0.48	16.64	9.24	16.49	0.01
Small (6 mm) diameter hole defect										
C_1^t	48.7	1848	53.44	54.74	C_4^r	51.6	1744	79.52	99.15	n/a
C_2^t	48.0	1875	60.00	50.08	C_5^r	50.8	1772	69.83	74.66	n/a
C_3^t	48.2	1867	55.27	46.12	C_6^r	51.2	1758	62.07	72.44	n/a
μ	48.3	1863	56.24	50.31	–	51.2	1758	70.47	82.08	–
σ	0.36	13.87	3.39	4.31	–	0.40	14.00	8.74	14.82	–
Large (13 mm) diameter hole defect										
C_1^t	49.2	1829	73.20	70.94	C_4^r	52.0	1731	64.69	77.06	n/a
C_2^t	48.3	1863	82.42	78.92	C_5^r	51.0	1765	96.41	111.36	n/a
C_3^t	48.2	1867	67.82	47.16	C_6^r	51.3	1754	60.52	67.74	n/a
μ	48.57	1853	74.48	65.67	–	51.43	1750	73.87	85.39	–
σ	0.55	20.88	7.38	16.52	–	0.51	17.35	19.63	22.97	–

Table 4: Calculated DSFs for softwood (pine) specimens (V^r/V^t = ratio of radial to tangential velocity).

No introduced defect									
Sample	Radial wave testing direction				Sample	Tangential wave testing direction				V^r/V^t
	t_f (μs)	V (m/s)	DSF_1	DSF_2		t_f (μs)	V (m/s)	DSF_1	DSF_2	
S_1	42.3	2128	85.41	82.51	S_1	71.0	1268	71.29	72.77	1.68
S_2	42.1	2138	66.01	71.53	S_2	70.4	1278	71.68	75.55	1.67
S_3	42.5	2118	65.32	67.86	S_3	68.5	1314	86.76	90.32	1.61
S_4	41.3	2179	61.33	71.66	S_4	64.7	1391	58.13	63.05	1.57
S_5	42.5	2118	80.01	85.90	S_5	69.9	1288	45.95	53.63	1.64
S_6	43.9	2050	94.45	106.68	S_6	69.6	1293	62.38	64.12	1.59
μ	42.43	2122	75.42	81.02	–	69.12	1305	66.03	69.91	1.63
σ	0.85	41.85	13.21	14.39	–	2.27	44.74	13.92	12.67	0.04
Small (6 mm) diameter hole defect										
S_1^t	42.5	2118	65.38	69.65	S_4^r	62.7	1435	65.74	68.92	n/a
S_2^t	42.6	2113	73.74	74.22	S_5^r	64.2	1402	56.43	62.81	n/a
S_3^t	42.8	2103	60.94	63.48	S_6^r	69.9	1288	64.49	66.06	n/a
μ	42.63	2111	66.69	69.12	–	65.6	1375	62.22	65.93	–
σ	0.15	7.64	6.50	5.39	–	3.80	77.13	5.05	3.06	–
Large (13 mm) diameter hole defect										
S_1^t	42.3	2128	65.52	65.48	S_4^r	62.0	1452	56.29	59.26	n/a
S_2^t	42.7	2108	69.43	71.39	S_5^r	62.7	1435	48.80	57.29	n/a
S_3^t	42.8	2103	65.69	65.37	S_6^r	69.7	1291	73.91	73.12	n/a
μ	42.6	2113	66.88	67.41	–	64.8	1393	59.67	63.22	–
σ	0.26	13.23	2.21	3.44	–	4.26	88.46	12.89	8.63	–

in the tangential direction, and while the right halves show tangential testing with radial holes. This enables easy comparison of the effect of the introduced damage. A statistical analysis of data in each column has been carried out and the mean and standard deviation of each column have been presented in the Tables.

The time of flight and effective wave velocity (which is just the specimen width—90 mm in this case—divided by the time of flight) are included as they are directly output by the Pundit PL 200 and are a very widely used measures in ultrasonic testing. The premise on which these are commonly used as damage indicators is that the wave velocity (for a given density) relates directly to the elastic modulus, hence, if referenced to a benchmark, is a useful measure of the average material quality. However, we see in all three tables that in each direction the change in velocity when damage is introduced is indiscernible above the variation in velocity between nominally identical samples. Furthermore there is considerable difference between different species, and even between the radial and tangential directions within the same sample (by a factor of 1.63 (mean value) for the softwood—the difference in the longitudinal direction for both species would be even greater), so that no meaningful results are obtainable. The problem here is that there has been no change to the material apart from drilling a hole, which is quite small relative to both the cross section size (90 mm) and the acoustic wavelength (around 24–39 mm depending on the specimen). There is no doubt that time of flight could still be a meaningful measure of damage in situations where large internal areas of the wood are beginning to rot for example.

Consider now the results for the proposed DSFs.

4.2. Hardwood

Figure 4 shows the box and whisker plots[1] corresponding to the statistics of DSF_1 for hardwood specimens when damage is introduced progressively. We see that without exception the mean value of DSF_1 increases when the small hole is introduced. In fact (refer to Table 2) the smallest DSF_1 of any sample with a hole present is larger than the largest DSF_1 of any intact specimen. And with only the exception of H_6^t, DSF_1 increases further when the hole is enlarged.

DSF_1 is therefore unambiguously detecting damage in the hardwood specimens.

In terms of using the filtered signal, the results for DSF_2 are presented both in Table 2 and box and whisker plots of Figure 4. Accordingly one can see that results are quite insignificantly affected by the filtering of the high frequency noise, where the increasing trend of the DSF_2 with

[1] In these plots the extremes of the 'box' represent the 25th and 75th percentiles respectively while the central mark indicates the median, and the 'whiskers' represent the most extreme data points not considered outliers.

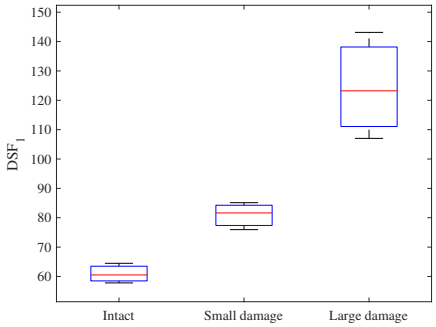

(a) DSF_1: Radial test—tangential damage

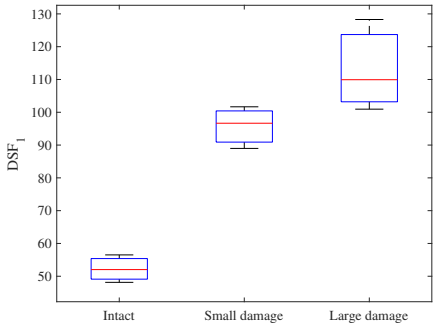

(b) DSF_1: Tangential test—radial damage

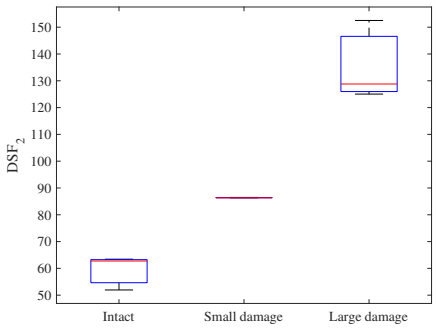

(c) DSF_2: Radial test—tangential damage

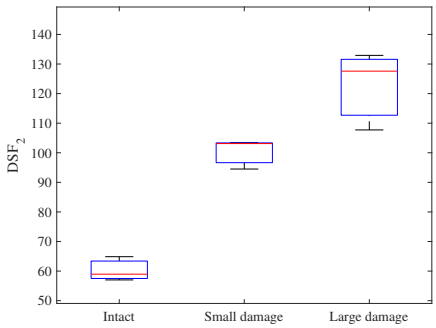

(d) DSF_2: Tangential test—radial damage

Figure 4: Box and whisker plots of DSF_1 and DSF_2 for the intact and artificially damaged hardwood specimens without pre-existing crack in tests conducted across both radial and tangential directions.

respect to the damage severity is perfectly preserved.

4.3. Hardwood with pre-existing cracks

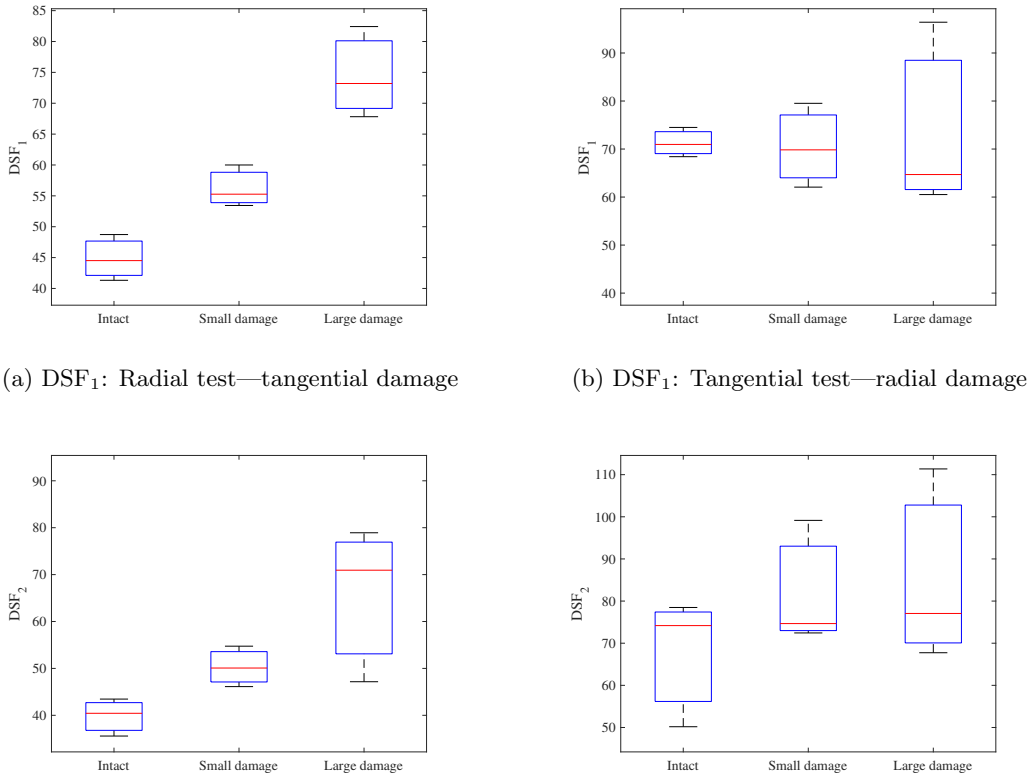

(a) DSF_1: Radial test—tangential damage

(b) DSF_1: Tangential test—radial damage

(c) DSF_2: Radial test—tangential damage

(d) DSF_2: Tangential test—radial damage

Figure 5: Box and whisker of DSF_1 and DSF_2 for the intact and artificially damaged hardwood specimens with pre-existing crack in tests conducted across both radial and tangential directions.

Table 3 and box and whisker plots of Figure 5 present respectively results of further tests conducted on another set of hardwood specimens and their corresponding statistic values that have natural splits in radial direction, designated C_i. Thus, they have pre-existing damage somewhat equivalent to the radial holes.

When tested with wave propagation in the radial direction, DSF_1 for the C specimens was in the range 40–50 with no introduced hole, increasing to 53–60 for the small tangential hole and 67–80 for the large tangential hole (samples C_1^t–C_3^t). These results are just a little lower than for the solid hardwood (H_i) specimens, but still show a very clear increase with damage severity. Thus the radial cracks appear to have had only a small effect on the overall magnitude when testing in the radial direction, and did not upset the clear trend between DSF_1 and damage severity.

On the other hand, for testing in the tangential direction there is no longer a clear trend of

DSF_1 with hole size, and there is a lot of variation between nominally similar specimens. This is because the cracks themselves (in addition to the introduced holes) represent damage that has been detected by DSF_1. Furthermore, the crack damage (being natural) is variable between samples and clearly significant compared with the introduced holes. Therefore it is fully to be expected that the tangential wave direction result show significant variation and no clear trend with the introduced damage size. Unfortunately as the cracks are naturally formed it is not possible to quantify them, hence the tests in this case can only validate the relationship of DSF_1 to the presence of damage, not to its severity.

It can be concluded therefore that DSF_1 continues to be a good damage indicator for these hardwood samples. Similarly again, Table 3 and Figure 5 show the sensitivity of the proposed method to noise to be negligible, as evident from the results for DSF_2.

4.4. Softwood

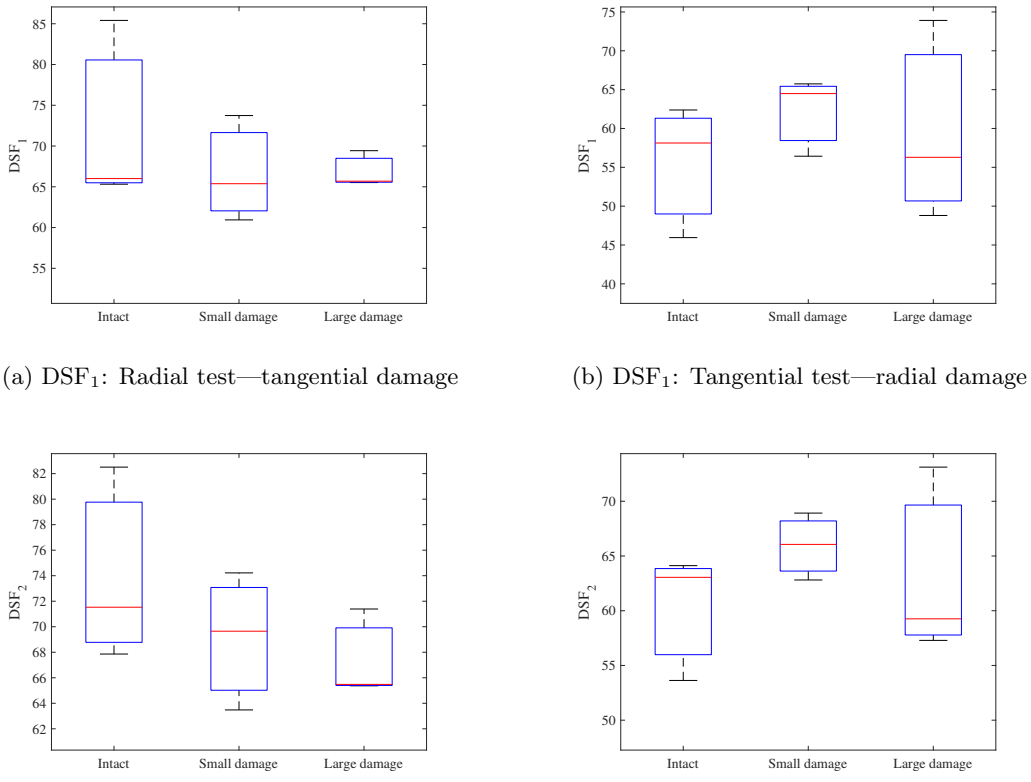

(a) DSF_1: Radial test—tangential damage

(b) DSF_1: Tangential test—radial damage

(c) DSF_2: Radial test—tangential damage

(d) DSF_2: Tangential test—radial damage

Figure 6: Box and whisker plots of DSF_1 and DSF_2 for the intact and artificially damaged softwood specimens in tests conducted across both radial and tangential directions.

As can be seen from the results in Table 4 and box and whisker plots of Figure 6, DSF_1 relates less clearly to the damage presence than for the hardwood specimens. However, even

though the detection is less successful, the DSF_2 results show that the detection method is still insensitive to any high frequency noise in the detected ultrasonic signal.

Further work is recommended to adapt the proposed DSF to softwoods. One possible explanation for the difference in behaviour is the significantly greater difference between the radial and tangential moduli of elasticity in the softwood versus the hardwood (as evident from the greater difference in wave propagation velocity). This is a question that numerical modelling may help to explore.

5. Conclusion

In this paper, a method is proposed and tested for characterising hole defects in woods using the signal recorded from an ultrasonic test. The signal is first decomposed into its constructive modes using EMD. Then, for damage detection, a DSF is proposed as the largest eigenvalue of the covariance matrix corresponding to all IMFs except the residual IMF. Two versions are presented: DSF_1 derived from the noisy ultrasonic signal, and DSF_2 corresponding to the same DSF derived from the filtered signal using a low-pass filter with a cutoff frequency 500 kHz. Both softwood and hardwood are studied in this paper. Several tests in both intact and damaged specimens have been conducted across the radial and tangential directions. The key findings of this study can be summarised as follows:

1. the proposed DSF proves to be highly successful in consistently and unambiguously identifying damage in hardwood specimens;
2. the DSF is able to identify both introduced holes and natural cracks, and correlates clearly with the size of the introduced damage;
3. results in softwood specimens were not conclusive, and further work is recommended for this application;
4. It has been shown that the proposed damage detection strategy is insensitive to noise, as in almost all of the cases the trend of the change in DSF is very closely preserved when a low-pass filter is applied.

A longer term objective is to investigate standing live trees, in which neither density nor moisture content can be reliably measured or controlled throughout the full trunk thickness by non-destructive methods. Therefore the paper has focused on detecting damage using damage sensitive features that do not rely on measurement of these quantities.

This paper has mainly focused on characterising hole defects in wooden sections, but has also been shown to be successful in identifying natural cracks. However, more investigation of the robustness of the proposed DSF for characterising other types of damage in woods is

recommended as the subject of future work, as well as to explore the effect of sample geometry on damage detection using the proposed DSF. Further work could also include numerical simulations to provide a better understanding of the physical basis of the DSF, as well as application to other materials.

Acknowledgment

The authors acknowledge the support of the Australian Research Council Industrial Transformation Training Hub 'The Centre for Forest Value' http://www.utas.edu.au/arcforest-value.

References

References

[1] N. G. Bingel, Cost saving benefits of wood structure maintenance [for power overhead lines], in: Proceedings of ESMO'95-1995 IEEE 7th International Conference on Transmission and Distribution Construction, Operation and Live-Line Maintenance, IEEE, 1995, pp. 11–16.

[2] J. Li, U. Dackermann, M. Subhani, R&D of NDTs for timber utility poles in service-challenges and applications (extension for bridge sub-structures and wharf structures), in: Proceedings of the Workshop on Civil Structural Health Monitoring (CSHM-4), Bundesanstalt für Materialforschung und -prüfung (BAM), Berlin, Germany, 2012, pp. 6–8.

[3] S. Bandara, P. Rajeev, E. Gad, B. Sriskantharajah, I. Flatley, Damage detection of in service timber poles using Hilbert-Huang transform, NDT & E International (2019) 102141.

[4] EN 408:2010+A1:2012 – Timber structures, Structural timber and glued laminated timber, Determination of some physical and mechanical properties, Standard, European Standards (2010).

[5] U. Dackermann, R. Elsener, J. Li, K. Crews, A comparative study of using static and ultrasonic material testing methods to determine the anisotropic material properties of wood, Construction and Building Materials 102 (2016) 963–976.

[6] M. Mori, M. Hasegawa, J.-C. Yoo, S.-G. Kang, J. Matsumura, Nondestructive evaluation of bending strength of wood with artificial holes by employing air-coupled ultrasonics, Construction and Building Materials 110 (2016) 24–31.

[7] B. İpekoğlu, An architectural evaluation method for conservation of traditional dwellings, Building and environment 41 (3) (2006) 386–394.

[8] H. Cruz, D. Yeomans, E. Tsakanika, N. Macchioni, A. Jorissen, M. Touza, M. Mannucci, P. B. Lourenço, Guidelines for on-site assessment of historic timber structures, International Journal of Architectural Heritage 9 (3) (2015) 277–289.

[9] M. M. Conde, C. R. Liñán, P. R. de Hita, Use of ultrasound as a nondestructive evaluation technique for sustainable interventions on wooden structures, Building and Environment 82 (2014) 247–257.

[10] V. Bucur, Nondestructive characterization and imaging of wood, Springer Science & Business Media, 2013.

[11] W. Li, J. Van den Bulcke, D. Mannes, E. Lehmann, I. De Windt, M. Dierick, J. Van Acker, Impact of internal structure on water-resistance of plywood studied using neutron radiography and X-ray tomography, Construction and Building Materials 73 (2014) 171–179.

[12] G. López, L. A. Basterra, L. Acuña, Estimation of wood density using infrared thermography, Construction and Building Materials 42 (2013) 29–32.

[13] E. Blomme, D. Bulcaen, F. Declercq, Air-coupled ultrasonic nde: experiments in the frequency range 750 kHz–2 MHz, NDT & E International 35 (7) (2002) 417–426.

[14] A. C. Senalik, G. Schueneman, R. J. Ross, Ultrasonic-based nondestructive evaluation methods for wood: a primer and historical review, USDA Forest Service, Forest Products Laboratory, General Technical Report, FPL-GTR-235, 2014; 36 p. 235 (2014) 1–36.

[15] T. Goto, Y. Tomikawa, S. Nakayama, T. Furuno, Changes of propagation velocity of ultrasonic waves and partial compression strength of decay-treated woods relationship between decrease of propagation velocity of ultrasonic waves and remaining strength, Mokuzai Gakkaishi 57 (6) (2011) 359–369.

[16] S. Lee, S.-J. Lee, J. S. Lee, K.-B. Kim, J.-J. Lee, H. Yeo, Basic study on nondestructive evaluation of artificial deterioration of a wooden rafter by ultrasonic measurement, Journal of Wood Science 57 (5) (2011) 387–394.

[17] F. Tallavo, G. Cascante, M. D. Pandey, A novel methodology for condition assessment of wood poles using ultrasonic testing, NDT & E International 52 (2012) 149–156.

[18] T. Mori, Y. Yanase, K. Tanaka, K. Kawano, Y. Noda, M. Mori, H. Kurisaki, K. Komatsu, Evaluation of compression and bending strength properties of wood damaged from biodeterioration, Journal of the Society of Materials Science, Japan 62 (4) (2013) 280–285.

[19] S.-J. Lee, S. Lee, S.-J. Pang, C.-K. Kim, K.-M. Kim, K.-B. Kim, J.-J. Lee, Indirect detection of internal defects in wooden rafter with ultrasound, Journal of the Korean Wood Science and Technology 41 (2) (2013) 164–172.

[20] A. Ettelaei, M. Layeghi, H. Z. Hosseinabadi, G. Ebrahimi, Prediction of modulus of elasticity of poplar wood using ultrasonic technique by applying empirical correction factors, Measurement 135 (2019) 392–399.

[21] M. Hirao, H. Ogi, EMATs for science and industry: noncontacting ultrasonic measurements, Springer Science & Business Media, 2013.

[22] L. Drain, Laser ultrasonics techniques and applications, Routledge, 2019.

[23] W. Grandia, C. Fortunko, Nde applications of air-coupled ultrasonic transducers, in: 1995 IEEE Ultrasonics Symposium. Proceedings. An International Symposium, Vol. 1, IEEE, 1995, pp. 697–709.

[24] Y. Fang, L. Lin, H. Feng, Z. Lu, G. W. Emms, Review of the use of air-coupled ultrasonic technologies for nondestructive testing of wood and wood products, Computers and electronics in agriculture 137 (2017) 79–87.

[25] D. Chimenti, Review of air-coupled ultrasonic materials characterization, Ultrasonics 54 (7) (2014) 1804–1816.

[26] T. Marhenke, J. Neuenschwander, R. Furrer, J. Twiefel, J. Hasener, P. Niemz, S. J. Sanabria, Modeling of delamination detection utilizing air-coupled ultrasound in wood-based composites, NDT & E International 99 (2018) 1–12.

[27] D. Pines, L. Salvino, Structural health monitoring using empirical mode decomposition and the Hilbert phase, Journal of Sound and Vibration 294 (1-2) (2006) 97–124.

[28] N. Cheraghi, F. Taheri, A damage index for structural health monitoring based on the empirical mode decomposition, Journal of Mechanics of Materials and Structures 2 (1) (2007) 43–61.

[29] N. E. Huang, Z. Shen, S. R. Long, M. C. Wu, H. H. Shih, Q. Zheng, N.-C. Yen, C. C. Tung, H. H. Liu, The empirical mode decomposition and the Hilbert spectrum for nonlinear and non-stationary time series analysis, Proceedings of the Royal Society of London A: Mathematical, Physical and Engineering Sciences 454 (1998) 903–995. doi:10.1098/rspa.1998.0193.

[30] J. Echeverria, J. Crowe, M. Woolfson, B. Hayes-Gill, Application of empirical mode decomposition to heart rate variability analysis, Medical and Biological Engineering and Computing 39 (4) (2001) 471–479.

[31] J.-C. Nunes, E. Deléchelle, Empirical mode decomposition: Applications on signal and image processing, Advances in Adaptive Data Analysis 1 (01) (2009) 125–175.

[32] Z. Liu, H. Wang, S. Peng, Texture classification through directional empirical mode decomposition, in: Proceedings of the 17th International Conference on Pattern Recognition, 2004. ICPR 2004., Vol. 4, IEEE, 2004, pp. 803–806.

[33] W.-F. Sun, Y.-H. Peng, J.-H. Xu, A de-noising method for laser ultrasonic signal based on EMD [J], Journal of Shandong University (Engineering Science) 5 (2008).

[34] Y.-K. Luo, S.-T. Luo, F.-L. Luo, M.-C. Pan, Realization and improvement of laser ultrasonic signal denoising based on empirical mode decomposition, Optics and Precision Engineering 2 (2013).

[35] T.-L. Chen, P.-W. Que, Q. Zhang, Q.-K. Liu, Ultrasonic signal identification by empirical mode decomposition and hilbert transform, Review of Scientific Instruments 76 (8) (2005) 085109.

[36] Y. Zhang, L. Yang, J. Fan, Study on feature extraction and classification of ultrasonic flaw signals, WSEAS Trans. Math 9 (2010) 529–538.

[37] N. El Karoui, Recent results about the largest eigenvalue of random covariance matrices and statistical application, Acta Physica Polonica Series B 36 (9) (2005) 2681.

[38] Z. Zhou, W. Wu, S. Wu, K. Jia, P.-H. Tsui, Empirical mode decomposition of ultrasound imagingfor gain-independent measurement on tissue echogenicity: A feasibility study, Applied Sciences 7 (4) (2017) 324.

[39] R. A. Horn, C. R. Johnson, Matrix analysis, Chapter one (Eigenvalues, Eigenvectors and Similarity), Cambridge University Press, 2012.

[40] M. Taskhiri, M. Hafezi, R. Harle, D. Williams, P. Turner, Ultrasonic and thermal testing to non-destructively identify internal defects in plantation eucalypts computers and electronics in agriculture, Computers and Electronics in Agriculture (in press) (2020).